

Article

A Novel Choice Procedure of Magnetic Component Values for Phase Shifted Full Bridge Converters with a Variable Dead-Time Control Method

Lei Zhao *, Haoyu Li, Yanxue Yu † and Yantian Wang †

School of Electrical Engineering and Automation, Harbin Institute of Technology, Harbin 150001, China; E-Mails: lihy@hit.edu.cn (H.L.); yanxueyu2015@gmail.com (Y.Y.); werya2015@gmail.com (Y.W.)

† These authors contributed equally to this work.

* Author to whom correspondence should be addressed; E-Mail: zhaoleihitee@gmail.com; Tel./Fax: +86-451-8641-2811.

Academic Editor: Thorsten Staake

Received: 12 May 2015 / Accepted: 26 August 2015 / Published: 4 September 2015

Abstract: Magnetic components are important parts of the phase shifted full bridge (PSFB) converter. During the dead-time of switches located in the same leg, the converter can achieve zero-voltage-switching (ZVS) by using the energies stored in magnetic components to discharge or charge the output capacitances of switches. Dead-time is usually calculated under a given set of pre-defined load condition which results in that the available energies are insufficient and ZVS capability is lost at light loads. In this paper, the PSFB converter is controlled by variable dead-time method and thus full advantage can be taken of the energies stored in magnetic components. Considering that dead-time has a great effect on ZVS, the relationship between available energies and magnetic component values is formulated by analyzing the equivalent circuits during dead-time intervals. Magnetic component values are chosen based on such relationship. The proposed choice procedure can make the available energies greater than the required energies for ZVS operation over a wide range of load conditions. Moreover, the burst mode control is adopted in order to reduce the standby power loss. Experimental results coincide with the theoretical analysis. The proposed method is a simple and practical solution to extend the ZVS range.

Keywords: phase shifted full bridge; dead-time; zero-voltage switching; wide range of load; high efficiency; standby condition

1. Introduction

By using parasitic circuit elements such as junction capacitances of switches and leakage inductance of transformer, phase-shifted full-bridge (PSFB) converter provides zero-voltage-switching (ZVS) for switches without requiring any additional active devices [1,2]. These characteristics can reduce switching loss and enable high switching frequency operation. Such advantages make the PSFB converter well suited for high efficiency, high power density and high reliability applications [3,4]. The circuit diagram of a PSFB converter is shown in Figure 1 [5,6]. T_r is the transformer which can be used as electric isolation and energy conversion. L_m is the magnetizing inductance of T_r . L_{lk} is the resonant inductance which includes the leakage inductance of T_r and an external inductance added to extend the ZVS range. L_o is the output filter inductance. As shown in Figure 1, magnetic components are important parts of the converter and they determine the operation modes and size of the converter [7–9].

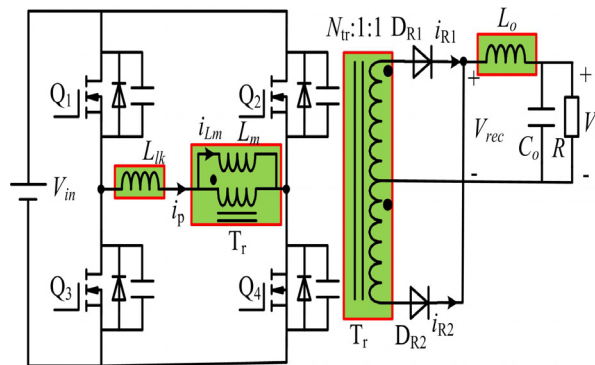


Figure 1. Circuit diagram of a phase-shifted full-bridge (PSFB) converter.

The drawback of PSFB converter is the dependency of ZVS characteristic on load conditions. ZVS is lost at light loads since energies which are stored in magnetic components are insufficient to fully discharge the output capacitances of switches. The loss of ZVS results in high Electromagnetic Interference (EMI) and low efficiency due to the increase of switching loss. The methods proposed in [10–13] can extend the ZVS range by adding auxiliary circuits which provide enough energies to achieve complete ZVS for all switches. Several methods to improve the efficiency of PSFB converter have been proposed, especially under light load conditions, with no additional devices. By properly selecting magnetizing inductance and resonant inductor [14], ZVS operation can be maintained in all capacity loads. The converter achieves high light-load efficiency with a penalty on the heavy-load efficiency. By adjusting switching control technique of full-bridge converter [15], the efficiency improvement can be up to 20%. However, switches operate with hard switching. The methods shown in [16,17] can reduce switching loss by changing dead-time and thus the light load efficiency can be improved.

In order to avoid overshooting, dead-time is needed between switches located in the same leg. Dead-time is a key parameter that needs to be optimized during the converter design. In the conventional design procedure, dead-time is constant regardless of load conditions, which results in additional loss due to the switch body diode reverse recovery and conduction. During dead-time of the PSFB converter, ZVS operation is achieved by using the energies stored in magnetic components to discharge and charge the output capacitances of switches. Dead-time is usually calculated under a

given set of pre-defined load conditions. As a result, the available energies are insufficient and ZVS capability is lost at light loads.

Standby power is electricity consumed by an appliance while it doesn't perform its primary function. A typical family, often having 20 devices, constantly draws standby power which is responsible for 5%–10% of the total power loss. The International Energy Agency (IEA) has proposed the one-watt plan, and the participating countries seek to lower standby power loss to below 1 watt in all products. To minimize the power consumption of power supplies in standby mode, some techniques have been proposed in [15].

In this paper, the detailed circuit analysis of PSFB converter during dead-time is performed. According to the analysis results, magnetic component and dead-time values have a great effect on the range of ZVS. Dead-time value needs to be varied with the load current so that the energies stored in magnetic components can be taken full advantage of. In order to ensure that the available energies are always greater than the required energies for ZVS operation over a wide range of loads, magnetic component values are chosen based on circuit analysis results during dead-time. Such choice procedure can extend the ZVS range and improve the light-load efficiency of PSFB converter. Moreover, the converter is controlled by burst mode under standby condition and the standby power loss is less than 1 watt.

This paper is organized as follows: a detailed circuit analysis during dead-time is presented in Section 2. Section 3 discusses the relationships between the available energies for ZVS and values of magnetic components. The proposed choice procedure of magnetic component values and control system are described in Section 4. In Section 5, experimental results are presented and discussed. The conclusions are given in Section 6.

2. Circuit Analysis

As load current decreases, the current through the output filter inductor will be discontinuous. The operation principle of PSFB converter in discontinuous current mode (DCM) is different from that in continuous current mode (CCM). The operation principles of the PSFB converter have been discussed in [5,6]. Figure 2 shows the steady waveforms in different modes and the key values can be calculated as follows.

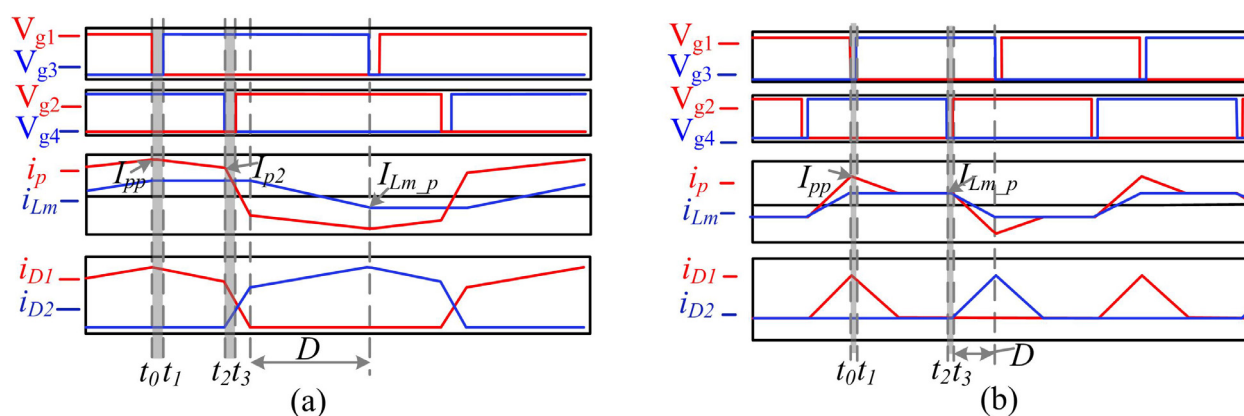


Figure 2. Key waveforms in different modes: (a) Continuous current mode (CCM); (b) Discontinuous current mode (DCM).

The duty cycle of primary voltage which is set by the controller, can be expressed as:

$$D = \begin{cases} \frac{N_{tr} V_o}{V_{in}} & \text{CCM} \\ \sqrt{\frac{4L_o I_o f_s V_o N_{tr}^2}{V_{in}(V_{in} - V_o N_{tr})}} & \text{DCM} \end{cases} \quad (1)$$

The peak value of primary current I_{pp} which corresponds to the output filter inductor current reflected to the primary side is described as:

$$I_{pp} = \begin{cases} \frac{I_o + \Delta I_{out}}{N_{tr}} + I_{Lm_p} & \text{CCM} \\ 2\Delta I_{out} + I_{Lm_p} & \text{DCM} \end{cases} \quad (2)$$

where ΔI_{out} is the current ripple of L_o .

The peak value of magnetizing current is calculated as:

$$I_{Lm_p} = \frac{DV_{in}}{4L_m f_s} \quad (3)$$

The primary current at t_2 in CCM operation is

$$I_{p2} = I_{pp} - V_o \frac{1-D}{2f_s N_{tr} L_o} \quad (4)$$

In order to ensure ZVS and avoid overshooting, dead-time is needed between the switches located in the same leg. During dead-time, ZVS is achieved by using the energy stored in magnetic components to discharge and charge the output capacitances of switches. The detailed circuit analysis during dead-time is presented as follows.

2.1. Circuit Analysis during the Dead-Time of Leading-Leg

Q_1 is turned off at t_0 and the primary current increases to I_{pp} . The output capacitances of Q_1 and Q_3 start to charge and discharge respectively. During the dead-time of leading-leg, the equivalent circuit of the converter in DCM operation is the same as that in CCM operation. Figure 3 shows the equivalent circuit and this circuit can be simplified as Figure 4. When the diode drawn with dashed line (the body diode of Q_3) comes into conduction in Figure 4, the switch Q_3 can be turned on with ZVS. In this interval, the filter inductor is transformed to the primary side and the primary current is regarded as a constant current source.

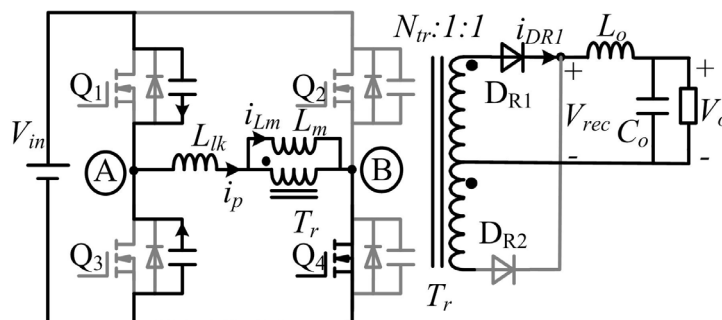


Figure 3. Equivalent circuit during $[t_0, t_1]$.

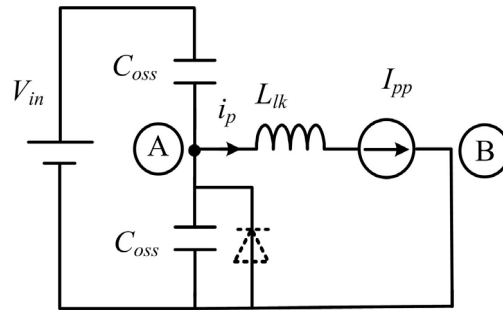


Figure 4. Simplified circuit during $[t_0, t_1]$.

2.2. Circuit Analysis during the Dead-Time of Lagging-Leg

Q_4 is turned off at t_2 and the converter starts to operate under the dead-time of lagging-leg condition. In order to analyze the effect of dead-time, it is assumed that dead-time is very wide. At the beginning of this transition, the rectifier diodes conduct at the same time. The summed current of D_{R1} and D_{R2} is equal to load current, the current of D_{R1} decreases while the current of D_{R2} increases. When the body diode of Q_2 comes into conduction, the transition is over. Depending on the load condition, the following three cases are possible during the lagging-leg transition [14]:

Case 1: The converter is in CCM operation and magnetizing current is smaller than the reflected load current. Resonance occurs between L_{lk} and output capacitances of Q_2 and Q_4 . D_{R1} and D_{R2} conduct at the same time and thus the transformer is shorted. Figure 5 shows the equivalent circuit which can be simplified as Figure 6.

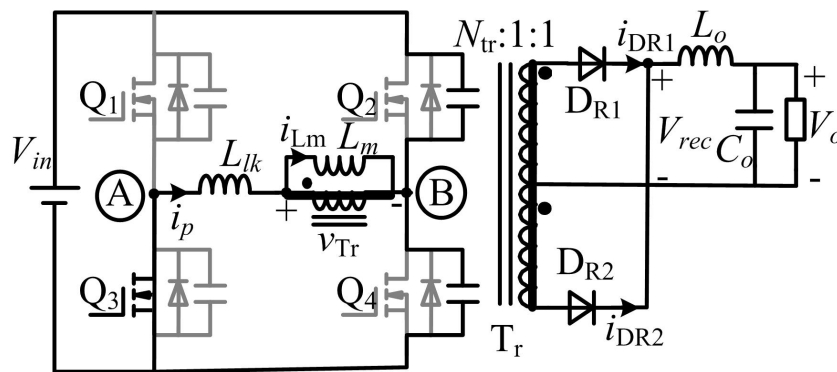


Figure 5. Equivalent circuit in Case 1.

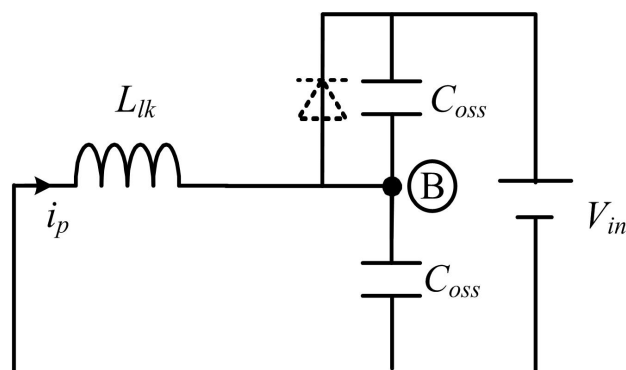


Figure 6. Simplified circuit in Case 1.

Case 2: The converter is in CCM operation and magnetizing current is larger than the reflected load current. The dead-time is wide while the converter still operates under the dead-time of lagging-leg condition. The transformer comes out of the shorted state and starts to transfer energy to the output side. Figure 7 shows the equivalent circuit in Case 2 and it can be simplified as Figure 8.

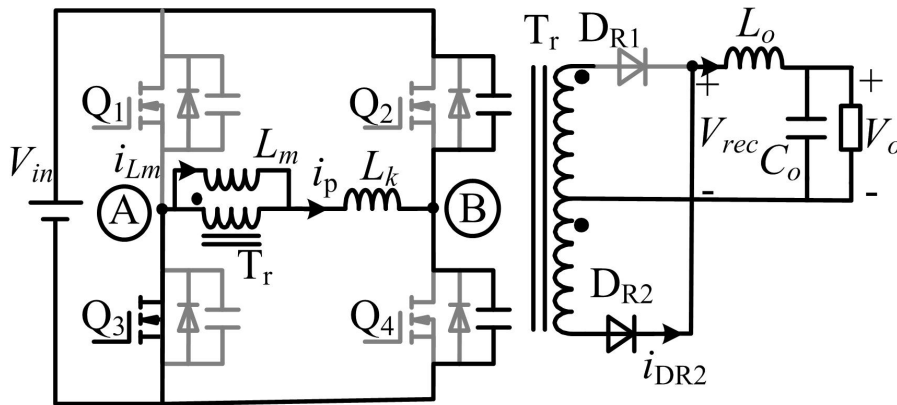


Figure 7. Equivalent circuit in Case 2.

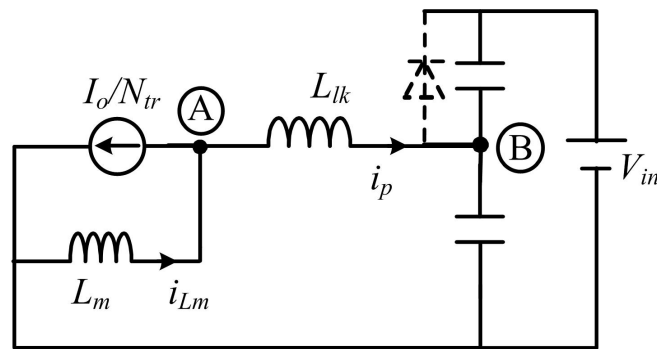


Figure 8. Simplified circuit in Case 2.

Case 3: The converter is in DCM operation. The current through L_o is zero and the rectifier diodes are turned off. Figure 9 shows the equivalent circuit in Case 3 and it can be simplified as Figure 10. The available energies to charge and discharge the capacitances are mainly stored in the magnetizing inductance.

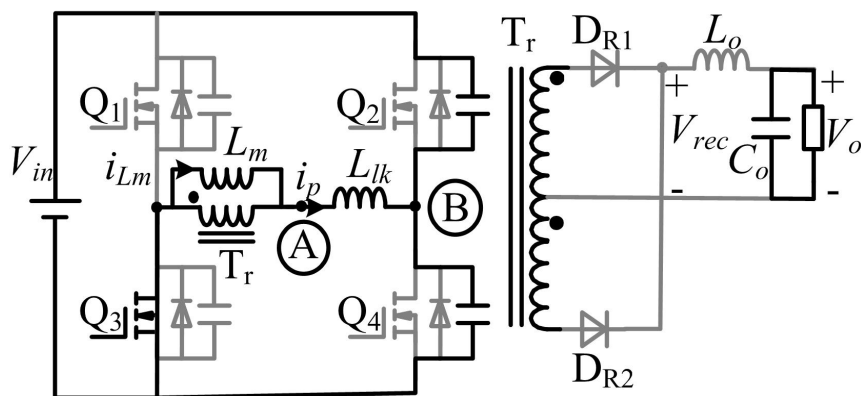


Figure 9. Equivalent circuit in Case 3.

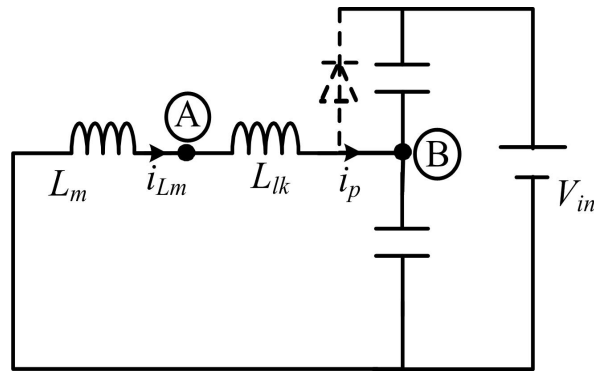


Figure 10. Simplified circuit in Case 3.

3. Available Energies for Zero-Voltage-Switching (ZVS) operation

The switch can achieve the ZVS operation during dead-time intervals by using the energies stored in magnetic components to force conduction of the switch’s body diode before turning the switch on. The available energies are related to the load condition which results in the ZVS characteristic loss at light loads.

As shown in Figure 4, the filter inductor is transformed to the primary side and the primary current is regarded as a constant current source to charge and discharge the output capacitances during the dead-time of leading-leg. The leading-leg switches can be turned on with ZVS easily. The required dead-time for leading-leg can be expressed as:

$$t_{Lead} = \frac{2C_{oss}V_{in}}{I_{pp}} \tag{5}$$

where C_{oss} is the output capacitance of the Metal-Oxide-Semiconductor-Field-Effect Transistor (MOSFET).

However, the lagging-leg switches are difficult to obtain ZVS operation since the filter inductor doesn’t participate in the transition. According to the circuit analysis during the dead-time of lagging-leg, the required energy E_{req} for completely charging and discharging the capacitances can be expressed as:

$$E_{req} = C_{oss}V_{in}^2 \tag{6}$$

As shown in Figure 6, only the energy stored in L_{lk} takes part in ZVS transition when the converter operates in Case 1 since the transformer is shorted. The available energy E_{Case1} can be expressed as follows:

$$E_{Case1} = \frac{1}{2}L_{lk}I_{P2}^2 \tag{7}$$

Figure 11 shows the available energy with various resonant inductances vs. load current. To realize ZVS operation, the available energy E_{Case1} should be larger than the required energy E_{req} . The condition can be expressed as:

$$I_O > I_{Case1} = \Delta I_{out} + V_{in}N_{tr}\sqrt{2C_{mos}/L_{lk}} - N_{tr}I_{Lm_p} \tag{8}$$

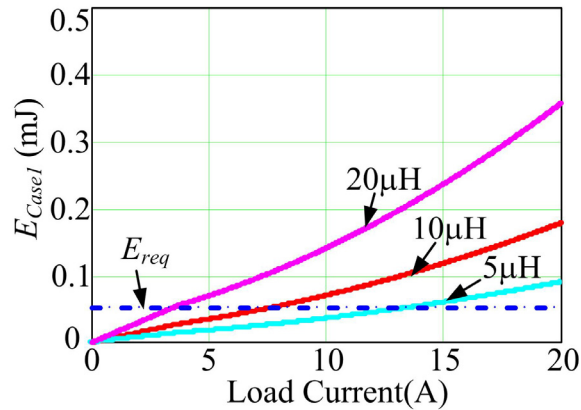


Figure 11. Available energy in Case 1 vs. load current.

As shown in Figure 11, the available energy increases with the value of L_{lk} . The ZVS range can be extended by using large resonant inductance. However, large resonant inductor reduces the effective duty cycle and increases both the conduction loss and voltage stress of the rectifier diodes. These disadvantages result in efficiency decay. The resonance between L_{lk} and C_{oss} provides a sinusoidal voltage across the switches. To ensure that all the energy stored in L_{lk} is available, the dead-time of lagging-leg t_{Lag} is set one fourth of the resonant period as follows:

$$t_{Lag} = 0.5\pi\sqrt{2L_{lk}C_{oss}} \tag{9}$$

At the beginning of lagging-lag dead-time, the transformer is shorted and the converter operates in Case 1. Only when the load current satisfies the following condition can Case 2 exist:

$$I_o < N_{tr}I_{Lm_p} \tag{10}$$

When the current of D_{R1} reaches zero, the converter operates in Case 2. From the simplified equivalent circuit of Figure 8, the energy stored in the magnetizing inductance can be used to provide ZVS and the available energy in Case 2 is:

$$E_{Case2} = \frac{1}{2}L_m(I_{Lm_p} - \frac{I_o}{N_{tr}})^2 + \frac{1}{2}L_{lk}I_{P2}^2 \tag{11}$$

Figure 12 shows the available energy vs. magnetizing inductance. Small magnetizing inductance results in large magnetizing current, therefore E_{Case2} increases while magnetizing inductance decreases. Dead-time should be enlarged since the magnetizing current is small and more time is needed to completely charge and discharge the capacitances. E_{Case2} should be larger than the required energy E_{req} . The condition for ZVS operation in Case 2 can be expressed as:

$$I_o < I_{Case2} = \frac{N_{tr}^2V_o}{4L_m f_s} - N_{tr}\sqrt{\frac{2E_{req}}{L_m}} \tag{12}$$

When the load current is smaller than ΔI_{out} , the converter enters in DCM operation. The critical load current between CCM and DCM can be calculated as follows:

$$I_{Cri} = \frac{D(V_{in}/N_{tr} - V_o)}{4f_s L_o} \tag{13}$$

As shown in Figure 10, both L_{lk} and L_m take part in ZVS transition in Case 3. Since L_{lk} is much smaller than L_m , the available energy in Case 3 is mainly stored in L_m , which is given by Equation (14).

$$E_{Case3} = \frac{L_o I_o V_o V_{in} N_{tr}^2}{8 L_m f_s (V_{in} - N_{tr} V_o)} \tag{14}$$

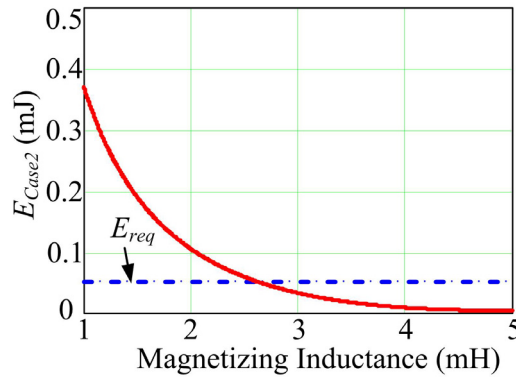


Figure 12. Available energy in Case 2 vs. magnetizing inductance.

Figure 13 shows the available energy in Case 3 vs. magnetizing inductance. The condition for ZVS operation in Case 3 can be expressed as:

$$I_o > I_{Case3} = \frac{4 V_{in} f_s L_m C_{oss}}{N_{tr} L_o} \left(\frac{V_m}{N_{tr} V_o} - 1 \right) \tag{15}$$

During dead-time in Case 3, the resonance between the magnetizing inductance and capacitances provides a sinusoidal voltage across the switches. The dead-time is set at one fourth of the resonant period.

$$t_{Lag} = 0.5\pi \sqrt{L_m C_{oss}} \tag{16}$$

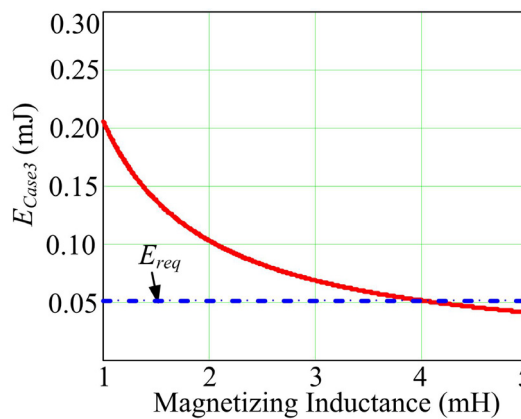


Figure 13. Available energy in Case 3 vs. magnetizing inductance.

4. Proposed Choice Procedure and Control Method

The PSFB converter can use the energies stored in magnetic components to discharge junction capacitances during dead-time and thus the switches can achieve ZVS. Figure 14 shows the stored energies and required energy for ZVS operation vs. load current. The drawback of PSFB converter is the dependency of ZVS characteristic on load condition. If the converter is controlled by the

conventional fixed dead-time method, only Case 1 exists during the lagging-leg dead-time. The available energy is stored in the resonant inductance while the magnetizing inductance doesn't take part in the ZVS transition. Only when the load current is greater than I_{Case1} , can the lagging-leg switches achieve ZVS operation. By carefully choosing magnetizing component values and adopting variable dead-time method, the energy stored in the magnetizing inductance can be used to provide ZVS transition energy and the ZVS range can be extended from I_{Case1} to I_{Case3} .

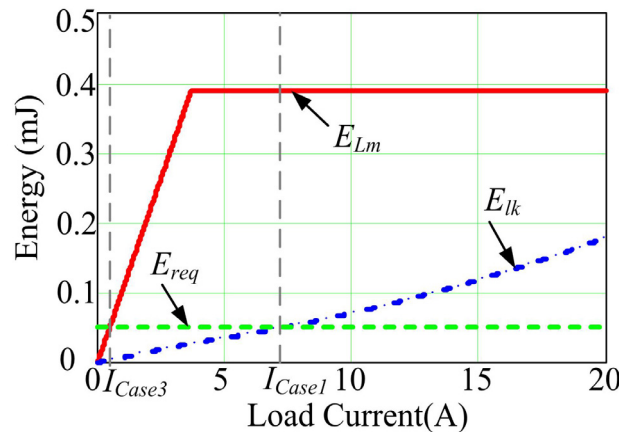


Figure 14. Stored energies and required energy vs. load current.

Three cases are possible during the dead-time of lagging-leg, as shown in Figure 15. By adopting the variable dead-time control method, the lagging-leg switches can achieve ZVS operation when load current locates in the colorful areas. If I_{Case2} is greater than I_{Case1} , the ZVS range of lagging-leg can be extended to I_{Case3} . According to Equations (8) and (12), the condition can be expressed as:

$$\left(\frac{1-D}{2N_{tr}^2}\right)\frac{L_m}{L_o} + \left(\frac{2\sqrt{2C_{oss}f_s}}{D}\right)\frac{L_m}{\sqrt{L_{lk}}} < 1 \tag{17}$$

L_o can reduce output voltage ripple and its value is usually calculated as follows:

$$L_o = \frac{D(V_{in}/N_{tr} - V_o)}{4f_s\Delta I_{out}} \tag{18}$$

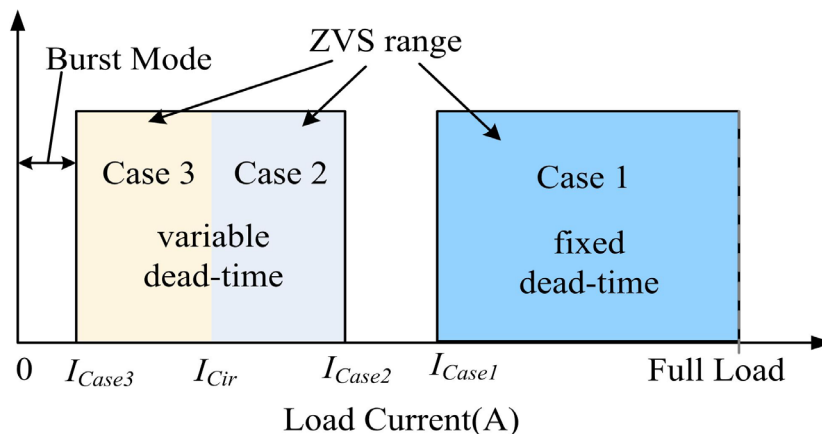


Figure 15. Operational modes with the variable dead-time control.

Figure 16 shows the proposed choice procedure of magnetic component values. ΔI_{out} is the current ripple of L_o and I_{Case3} is the minimum load current for ZVS operation, which are usually given by the converter designer. In general, ΔI_{out} is set at 20 percent of full load current and I_{Case3} is set at 1~3 percent.

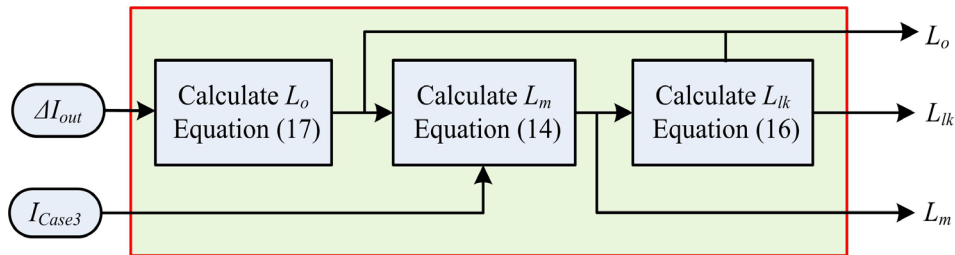


Figure 16. Block diagram of the proposed choice procedure.

Figure 17 shows the block diagram of the proposed control method. The control system consists of two individual control loops. The first loop regulates the output voltage by controlling the phase-shift angle. In order to balance the flux of transformer and improve dynamic response, peak current mode control (PCMC) is adopted. The proportional integral (PI) controller determines the peak current reference signal I_{ref} . Primary current i_p is compared with I_{ref} and then the output synchronizing signal (SYN) of the on-chip analog comparator determines the phase-shift angle. The second loop adjusts dead-time t_d and pulse width modulation (PWM) signals. According to the load current I_o , the controller adjusts t_d according to the following rules:

- (1) Under heavy loads (in Case 1), the available energies stored in L_{lk} is sufficient to provide ZVS for lagging-lag switches and t_d is equal to 300 ns.
- (2) When the load current locates in Case 2, the energy stored in magnetizing inductance can be used to charge and discharge capacitances by increasing t_d .
- (3) Under light loads (in Case 3), the converter enters into DCM. t_d is set at one fourth of the resonant period between magnetizing inductance and capacitances.

The converter enters into standby mode when the load current is less than I_{Case3} . In order to prevent bouncing between two switching modes, a hysteresis band is added. I_{burst} is the peak primary current when load current is I_{Case3} . When primary current beyond I_{burst} , $En = 1$, and the PWM module enables output. In contrast, $En = 0$, and the switching stops. Figure 18 shows the key waveforms with burst mode control. V_{ave} is the average output voltage under standby condition.

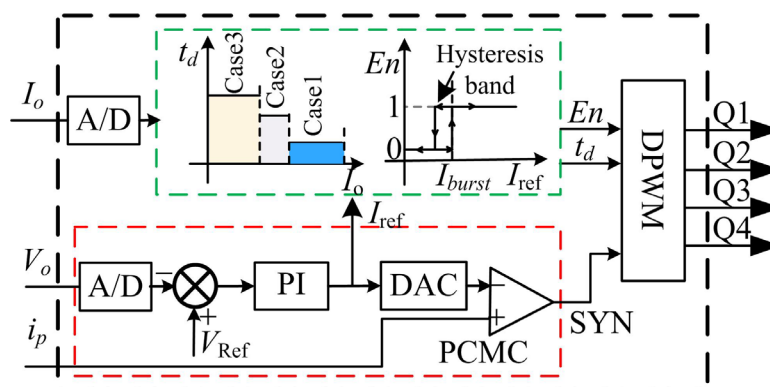


Figure 17. Control block diagram of the proposed method.

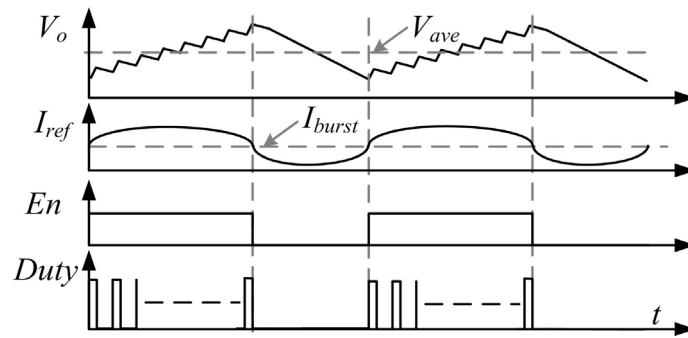


Figure 18. Key waveforms with burst mode control.

5. Experimental Results

A 1-kW prototype is implemented to verify the advantages of the proposed method. The Digital-Signal-Processing (DSP) TMS320F28027 (Texas Instruments, Dallas, TX, USA) is adopted for the digital control of the PSFB converter. Considering the performance of DSP and influence of limit-cycle, the switching frequency is selected as 50 kHz. The input voltage V_{in} is 400 V while the output voltage is 48 V. The turn ratio of transformer is 5:1:1, and rectifier diodes are STTH6002C. STW20NM60N is used as the primary switches and switching delay is 150 ns. The current ripple of L_o , ΔI_{out} , is 4 A and the minimum load current for ZVS operation, I_{Case3} , is 0.3 A. Based on the analysis of equations and the other specified parameters, the values of magnetic components and dead-time of lagging-leg are obtained. Table 1 shows the calculation results.

Table 1. Calculation results based on the proposed method.

Calculation Results	Magnetic Components			Dead-Time of Lagging-Leg		
Symbol	L_o	L_m	L_{lk}	Case 1	Case 2	Case 3
Value	25 μ H	1.5 mH	30 μ H	300 ns	700 ns	1.2 μ s

Figure 19 shows the waveforms of driver signals and voltage across Q_2 under different load conditions. By adopting the proposed choice procedure of magnetic component values, the lagging-leg switches are turned on with ZVS in all cases. The experimental results coincide with the theoretical analysis. The light-load efficiency of the converter with the proposed variable dead-time control method can be significantly improved since switching loss is dominant in Cases 2 and 3 operations.

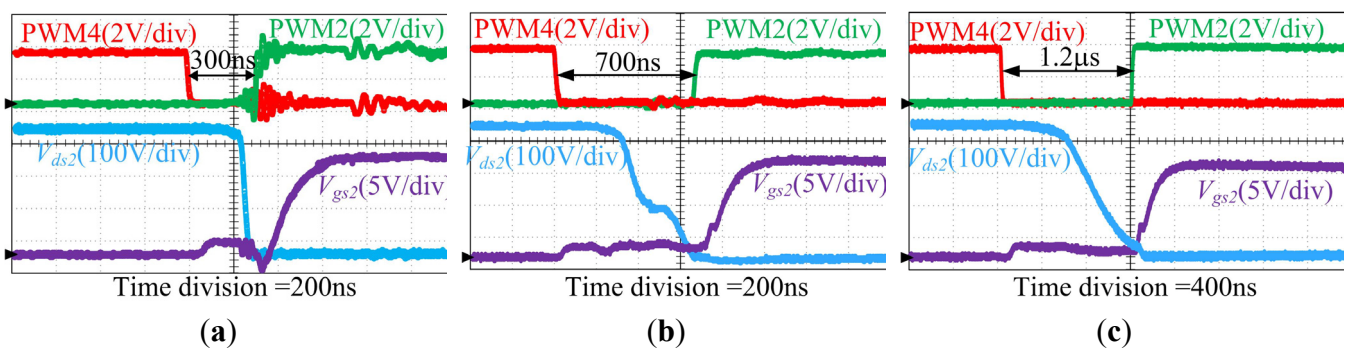


Figure 19. Experimental waveforms of Q_2 under different load conditions. (a) Case 1, $I_o = 20$ A; (b) Case 2, $I_o = 5$ A; (c) Case 3, $I_o = 0.5$ A.

Figure 20 shows the measured efficiencies with the variable and fixed dead-time methods. It is clearly visible that the light-load efficiency is significantly improved since all switches can achieve ZVS operation.

Figure 21 shows the key waveforms under standby condition. The proposed control method provides lower output voltage ripple as compared to the method shown in [15]. As shown in Figure 21, the equivalent switching frequency is significantly reduced by adopting burst mode. The standby power is 0.75 W and experiment result satisfies the requirement of “1 W plan”.

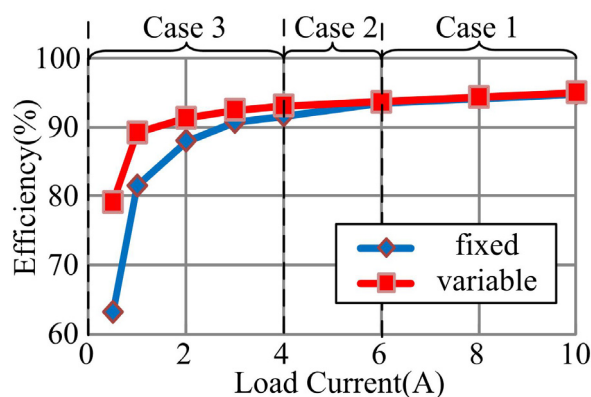


Figure 20. Measured efficiencies with different control methods.

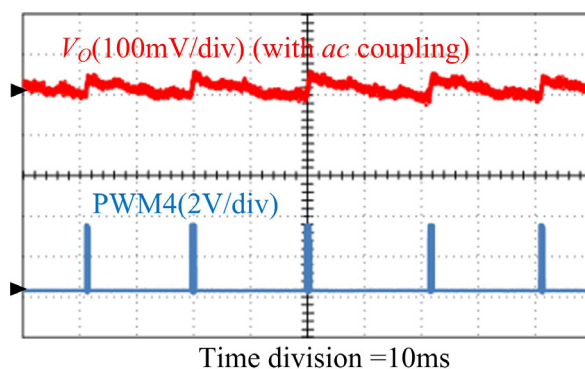


Figure 21. Key waveforms under standby condition.

6. Conclusions

By analyzing the equivalent circuits during dead-time intervals in a PSFB converter, a variable dead-time control method and choice procedure of magnetic component values are presented in this paper. The available energies stored in magnetic components are always greater than the required energy over a wide range of loads. The energy stored in magnetizing inductance can be taken full advantage of by adopting the variable dead-time control method and then all the switches can achieve ZVS under light load conditions. The proposed methods can extend the range of ZVS without requiring any additional devices. With the burst mode control method under standby condition, the equivalent switching frequency is reduced significantly and the standby power is less than 1 W. Experimental results coincide with the theoretical analysis. The proposed choice procedure and variable dead-time control method are simple and practical solutions for reducing the power loss under light load and standby conditions.

Acknowledgments

This work was supported by National Natural Science Foundation (Grant No.51074056) and Delta Environmental & Educational Foundation (Grant No.DREG2011006).

Author Contributions

Lei Zhao was responsible for the theoretical derivation and paper writing. Haoyu Li proposed the main idea and analysis method. Yanxue Yu and Yutian Wang carried out the simulation and verification.

Conflicts of Interest

The authors declare no conflict of interest.

References

1. Chen, Z.; Liu, S.; Shi, L. A soft switching full bridge converter with reduced parasitic oscillation in a wide load range. *IEEE Trans. Power Electron.* **2014**, *29*, 801–811.
2. Zhao, L.; Li, H.; Liu, Y.; Li, Z. High efficiency variable-frequency full-bridge converter with a load adaptive control method based on the loss model. *Energies* **2015**, *8*, 2647–2673.
3. Shi, X.; Jiang, J.; Guo, X. An efficiency-optimized isolated bidirectional DC-DC converter with extended power range for energy storage systems in microgrids. *Energies* **2013**, *6*, 27–44.
4. Lai, C.-M.; Yang, M.-J.; Liang, S.-K. A zero input current ripple ZVS/ZCS boost converter with boundary-mode control. *Energies* **2014**, *7*, 6765–6782.
5. Cho, B.H.; Sabate, J.A.; Vlatkovic, V.; Ridley, R.B.; Lee, F.C. Design Considerations for High-Voltage High-Power Full-Bridge Zero-Voltage-Switched PWM Converter. In Proceedings of the Fifth Annual Applied Power Electronics Conference and Exposition, Los Angeles, CA, USA, 11–16 March 1990; pp. 275–284.
6. Vlatkovic, V.; Sabate, J.A.; Ridley, R.B.; Lee, F.C.; Cho, B.H. Small-signal analysis of the phase-shifted PWM converter. *IEEE Trans. Power Electron.* **1992**, *7*, 128–135.
7. Petkov, R. Optimum design of a high-power, high-frequency transformer. *IEEE Trans. Power Electron.* **1996**, *11*, 33–42.
8. Lotfi, A.W.; Chen, Q.; Lee, F.C. A Nonlinear Optimization Tool for the Full-Bridge Zero-Voltage-Switched DC-DC Converter. In Proceedings of the Power Electronics Specialists Conference, Toledo, Spain, 29 June–3 July 1992; pp. 1301–1309.
9. Badstuebner, U.; Biela, J.; Kolar, J.W. An Optimized, 99% Efficient, 5kW, Phase-Shift PWM DC-DC Converter for Data Centers and Telecom Applications. In Proceedings of the 2010 International of Power Electronics Conference, Sapporo, Japan, 21–24 June 2010; pp. 626–634.
10. Kim, Y.D.; Cho, K.M.; Kim, D.-Y.; Moon, G.-W. Wide-range ZVS phase-shift full-bridge converter with reduced conduction loss caused by circulating current. *IEEE Trans. Power Electron.* **2013**, *28*, 3308–3316.
11. Chen, Z.; Liu, S.; Shi, L. Improved zero-voltage switching pulse width modulation full bridge converter with self-regulating auxiliary current. *IET Power Electron.* **2013**, *6*, 287–296.

12. Chen, Z.; Liu, S.; Ji, F. Power loss analysis and comparison of two full-bridge converters with auxiliary networks. *IET Power Electron.* **2012**, *5*, 1934–1943.
13. Jang, Y.; Jovanovic, M.M. A new PWM ZVS full-bridge converter. *IEEE Trans. Power Electron.* **2007**, *22*, 987–994.
14. Redl, R.; Balogh, L.; Edwards, D. Optimum ZVS Full-Bridge DC/DC Converter with PWM Phase-Shift Control: Analysis, Design Considerations, and Experimental Results. In Proceedings of the Applied Power Electronics Conference and Exposition, Orlando, FL, USA, 13–17 February 1994; pp. 159–165.
15. Chen, B.Y.; Lai, Y.S. Switching control technique of phase-shift-controlled full-bridge converter to improve efficiency under light-load and standby conditions without additional auxiliary components. *IEEE Trans. Power Electron.* **2010**, *25*, 1001–1012.
16. Kim, D.Y.; Kim, C.E.; Moon, G.W. Variable delay time method in the phase-shifted full-bridge converter for reduced power consumption under light load conditions. *IEEE Trans. Power Electron.* **2013**, *28*, 5120–5127.
17. Kim, J.W.; Kim, D.K.; Kim, C.E.; Moon, G.W. A simple switching control technique for improving light load efficiency in a phase-shifted full-bridge converter with a server power system. *IEEE Trans. Power Electron.* **2014**, *29*, 1562–1566.

© 2015 by the authors; licensee MDPI, Basel, Switzerland. This article is an open access article distributed under the terms and conditions of the Creative Commons Attribution license (<http://creativecommons.org/licenses/by/4.0/>).